J. Moscow Phys. Soc. 1 (1991) 391–406. Printed in the UK

The two-particle Green function in a model of a one-dimensional disordered system: An exact solution?

M V Sadovskii and A A Timofeev

Institute of Electrophysics, Ural Branch of the USSR Academy of Sciences, Komsomol'skaya ul. 34, 620219 Sverdlovsk, USSR

Received 4 July 1991

Abstract. The paper suggests an effective procedure for summing all Feynman diagrams for the two-particle Green function in a one-dimensional model with a Gaussian random field whose correlator is Lorentzian (in the momentum space) with its maximum at $Q = 2p_F$, with p_F the Fermi momentum. This model can be considered a Gaussian model of the Peierls transition (charge density and spin density waves) in a fluctuation region with a well-developed short-range order. The authors formulate a recurrence procedure for calculating the vertex part, which describes the response of the system to an external electromagnetic field, and obtain a general picture of the evolution of the frequency dependence of conductivity as a function of the short-range order correlation length, which describes absorption through a pseudogap and localization.

1. Introduction

There is only a limited number of models of the electronic properties of one-dimensional disordered systems that allow an exact solution [1, 2]. The interest in such models is due to the general problem of studying the electronic states in disordered systems and to specific problems of the physics of quasi-one-dimensional systems. Attention has especially focused on the manifestation of Anderson localization in the one-dimensional case for arbitrarily weak disorder [3–5]. Resolving this problem has proved extremely difficult since localization is determined by the properties of the two-particle Green function, about which very few exact statements are known.

The majority of exact results in the theory of one-dimensional disordered systems have been obtained by employing sophisticated mathematical techniques specially designed to describe one-dimensional problems and unsuitable for generalization to the multidimensional case. Only in a few cases have exact solutions been obtained via standard methods of the quantum theory of multiparticle systems [6]. Such models are of special interest primarily from the stand-point of checking the effectiveness of standard approximation methods. They could also lead to instructive results easily generalized to the multidimensional case.

A model of this kind was suggested some time ago by one of the present authors [7–9]. Within its framework it was established that the scattering of an electron on short-range order Gaussian fluctuations with a characteristic period determined by the wavevector $Q \propto 2p_F$ (p_F is the Fermi momentum) leads to the formation of a 'pseudogap' in the neighbourhood of the Fermi level that evolves

0960-0175/91/040391+16$03.50

with variations in the short-range order correlation radius [9]. In the approximation of large correlation radii there has also been obtained an exact analytical solution for the two-particle Green function describing, among other things, the absorption of electromagnetic radiation through the pseudogap [7, 8]. For the particular case of commensurate fluctuations a similar model was considered in Wonneberger and Lautenschlager [10]. The results obtained in these papers have been used to interpret the optical properties of quasi-one-dimensional systems undergoing a Peierls transition [8, 11] and in some other problems (e.g., see [12]). Lately a model of the same kind has been suggested for interpreting a number of properties of high-temperature superconductors [13–15]. The authors of [15] suggest a general recurrence procedure for calculating the two-particle Green function that is valid for arbitrary short-range correlation radii and allows for all the respective perturbation-theory diagrams.

The present paper is devoted to a thorough study of the solution used in [15], an analysis of its special features from the viewpoint of the theory of one-dimensional disordered systems, and a comparison of the 'exact' results with those obtained within the framework of standard approximation methods.

2. The model

We consider an electron placed in a Gaussian random field $\Delta(x)$ with a correlation function

$$\langle\Delta(x)\Delta(x')\rangle = \Delta^2 \exp\{-|x-x'|\,\xi^{-1}\}\cos[2p_F(x-x')] \tag{1}$$

where Δ^2 is the mean square of a field fluctuation, and ξ the short-range order correlation radius. Such a correlator appears, for instance, in fluctuations of the order parameter in the Ginzburg–Landau model for a Peierls transition [16]. In what follows Δ and ξ are considered parameters of the theory. The Fourier transform of (1) is

$$\begin{aligned}\langle\Delta_Q\Delta_{-Q}\rangle &\equiv \Delta^2 S(Q)\\ &= 2\Delta^2\left(\frac{\kappa}{(Q-2p_F)^2+\kappa^2}+\frac{\kappa}{(Q+2p_F)^2+\kappa^2}\right)\end{aligned} \tag{2}$$

with $\kappa = \xi^{-1}$. The simplest self-energy part of the one-electron Green function has the form (figure 1)

$$\begin{aligned}\Sigma(\varepsilon,p) &= \Delta^2\int\frac{dQ}{2\pi}\,\frac{S(Q)}{\varepsilon-\xi_{p-Q}-i\delta\,\mathrm{sgn}\,\xi_{p-Q}}\\ &\cong \frac{\Delta^2}{\varepsilon+\xi_p+iv_F\kappa\,\mathrm{sgn}\,\xi_p}\\ &\equiv \Delta^2 G_0(\varepsilon;-\xi_p-iv_F\,\mathrm{sgn}\,\xi_p)\qquad (p\propto p_F)\end{aligned} \tag{3}$$

where $\varepsilon_p \cong v_F(|p|-p_F)$, v_F is the Fermi velocity, and we have allowed for the fact that $\xi_{p-2p_F} = -\xi_p$.

We also consider the case of commensurate fluctuations [10], when $\xi_p = -W\cos(pa)$, with a the lattice constant, and $2p_F = \pi/a$ (half-filled bands, period

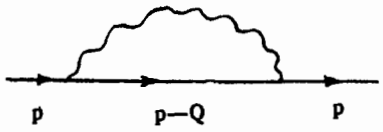

Figure 1. The simplest contribution to the self-energy part.

doubling). The diagram in figure 1 and the result of the (3) type were basic to the analysis conducted in [16]. In [7, 8] all Feynman diagrams for the one- and two-particle Green functions were summed for the asymptotic limit $\kappa \to 0$. An effective summation of all the diagrams for the one-particle Green function was carried out in [9] for arbitrary values of κ. In the nth order of the perturbation expansions in Δ^2 there are $n!$ diagrams in the case of incommensurate fluctuations and $(2n-1)!! = (2n-1)!/2^{n-1}(n-1)!$ in the case of commensurate fluctuations (period doubling) [9]. Figure 2 shows all the important diagrams of the third order in Δ^2 for the one-electron Green function in the incommensurate case. The rules for calculating the contributions of arbitrary diagrams have been thoroughly discussed in [9]. Generally, the contribution of any diagram is determined by the position of the 'initial' and 'final' vertexes for the interaction lines. Here to each one-electron line following the 'initial' vertex there is assigned (see equation (3)) an expression of the free-particle propagator type in which $iv_F\kappa \operatorname{sgn} \xi_p$ is added to the denominator, while in a similar line following the 'final' vertex this term is subtracted from the denominator. The integers in figure 2 stand for the number of such contributions in each of the corresponding denominators. The reader can easily see that the contribution of any diagram with crossed interaction lines can be uniquely represented by a respective diagram without crossed interaction lines, since their contributions are equal (e.g., in figure 2 diagram (d) provides the same contribution as diagram (e)). The general procedure for such assigning is given in [9], in accordance with the method first suggested by Elyutin [17]. Each vertex is assigned an integer equal to the number of terms $iv_F\kappa$ in the denominator of the electron line following the given vertex. The initial vertex is assigned the integer $N_n = N_{n-1}+1$, where N_{n-1} is the integer assigned to the closest vertex on the left. The final vertex is assigned the integer $N_{n-1} - 1$, where $N_0 = 0$ and n is the ordinal number of the vertex.

We introduce

$$v(k) = \begin{cases} (k+1)/2 & \text{if } k = 2m+1 \\ k/2 & \text{if } k = 2m \end{cases} \tag{4}$$

for the case of incommensurate fluctuations and

$$v(k) = k \tag{5}$$

for the case of commensurate fluctuations. It can easily be verified that the number of irreducible diagrams for the self-energy part that are equal to the given diagram without crossed interaction lines is given by the product of the factors $v(N_n)$ for all the initial vertexes of a given diagram. Hence, further analysis can be carried out in terms of diagrams without crossings, assigning to all initial vertexes the additional factors $v(N_n)$ [9, 17].

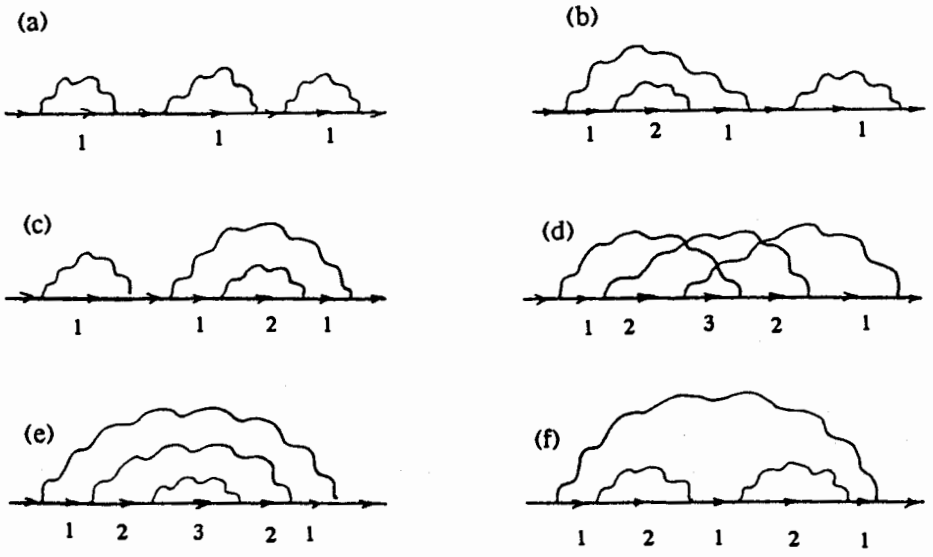

Figure 2. Δ^6-order diagrams for the Green function (the incommensurate case).

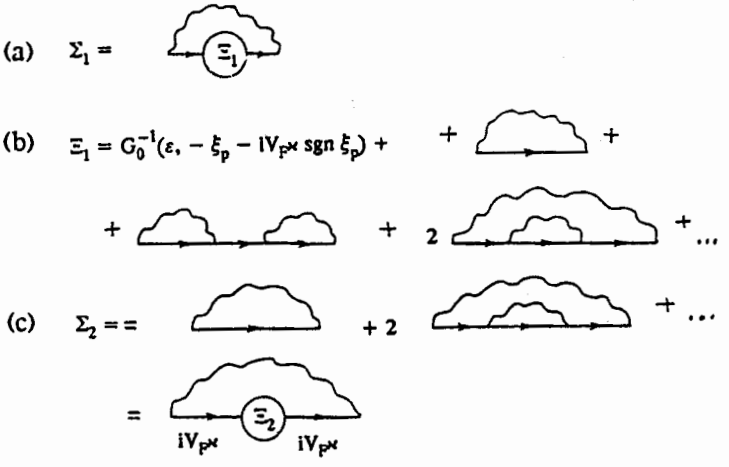

Figure 3. The diagrammatic structure of the recurrence procedure for the self-energy part.

Applying Elyutin's method makes it possible to build an exact representation for the one-electron Green function in the form of a continued fraction [9]. The structure of this solution is based on the ordinary Dyson equation

$$G^{-1}(\varepsilon,\xi_p) = G_0^{-1}(\varepsilon,\xi_p) - \Sigma_1(\varepsilon,\xi_p) \tag{6}$$

where for the self-energy part we have (figure 3(a))

$$\Sigma_1(\varepsilon,\xi_p) = \Delta^2\Xi_1(\varepsilon,\xi_p)\frac{v(1)}{(\varepsilon+\xi_p+\mathrm{i}v_F\kappa\,\mathrm{sgn}\,\xi_p)^2}$$
$$= \Delta^2 v(1)G_0^2(\varepsilon,-\xi_p-\mathrm{i}v_F\,\mathrm{sgn}\,\xi_p)\Xi_1(\varepsilon,\xi_p) \tag{7}$$

and for $\Xi_1(\varepsilon,\xi_p)$ we have the expansion depicted in figure 3(b), where there are no diagrams with crossed interaction lines but where the kth vertex (counting from the left) with an 'outgoing' line is assigned a combinatorial factor $v(k)$ (4) or (5), which allows taking into account the contributions of all the diagrams with crossed interaction lines. Respectively, $\Xi_1(\varepsilon,\xi_p)$ can be written as

$$\Xi_1(\varepsilon,\xi_p) = G_0^{-2}(\varepsilon,-\xi_p-\mathrm{i}v_F\kappa\,\mathrm{sgn}\,\xi_p)\frac{1}{G_0^{-1}(\varepsilon,-\xi_p-\mathrm{i}v_F\kappa\,\mathrm{sgn}\,\xi_p)-\Sigma_2(\varepsilon,\xi_p)} \tag{8}$$

where $\Sigma_2(\varepsilon,\xi_p)$ is expressed by the sum of irreducible diagrams shown in figure 3(c):

$$\Sigma_2(\varepsilon,\xi_p) = \Delta^2 v(2)G_0^2(\varepsilon,\xi_p+2\mathrm{i}v_F\kappa\,\mathrm{sgn}\,\xi_p)\Xi_2(\varepsilon,\xi_p) \tag{9}$$

$$\Xi_2(\varepsilon,\xi_p) = G_0^{-2}(\varepsilon,\xi_p+2\mathrm{i}v_F\kappa\,\mathrm{sgn}\,\xi_p)\frac{1}{G_0^{-1}(\varepsilon,\xi_p+2\mathrm{i}v_F\kappa\,\mathrm{sgn}\,\xi_p)-\Sigma_3(\varepsilon,\xi_p)} \tag{10}$$

etc. The final result is

$$\Sigma_k(\varepsilon,\xi_p) = \Delta^2 G_0^2\left(\varepsilon,(-1)^k(\xi_p+\mathrm{i}kv_F\kappa\,\mathrm{sgn}\,\xi_p)\right)v(k)\,\Xi_k(\varepsilon,\xi_p) \tag{11}$$

$$\Xi_k(\varepsilon,\xi_p) = G_0^{-2}\left(\varepsilon,(-1)^k(\xi_p+\mathrm{i}kv_F\kappa\,\mathrm{sgn}\,\xi_p)\right)$$
$$\times\frac{1}{G_0^{-1}\left(\varepsilon,(-1)^k(\xi_p+\mathrm{i}kv_F\kappa\,\mathrm{sgn}\,\xi_p)\right)-\Sigma_{k+1}(\varepsilon,\xi_p)} \tag{12}$$

$$\Sigma_k(\varepsilon,\xi_p) = \Delta^2 v(k)\frac{1}{G_0^{-1}\left(\varepsilon,(-1)^k(\xi_p+\mathrm{i}kv_F\kappa\,\mathrm{sgn}\,\xi_p)\right)-\Sigma_{k+1}(\varepsilon,\xi_p)}$$
$$\equiv \Delta^2 v(k)G_k(\varepsilon,\xi_p) \tag{13}$$

$$G_k(\varepsilon,\xi_p) = \left[\varepsilon-(-1)^k(\xi_p+\mathrm{i}kv_F\kappa\,\mathrm{sgn}\,\xi_p)-\Delta^2 v(k+1)G_{k+1}(\varepsilon,\xi_p)\right]^{-1} \tag{14}$$

with $G_{k=0}(\varepsilon,\xi_p) = G(\varepsilon,\xi_p)$. These recurrence relations yield an exact representation of the one-electron Green function in the form of a continued fraction. The results of numerical calculations of the corresponding electronic state density for different values of the short-range order correlation radius $\xi = \kappa^{-1}$ are given in [9]. The results exhibit, among other things, the formation of a pseudogap approximately 2Δ wide in

the vicinity of the Fermi level [7–11, 16] that gradually fills up (degrades) as ξ gets smaller.

Figures 4 and 5 illustrate the results of numerical calculations of the spectral density

$$A(\varepsilon,\xi_p)=\frac{1}{\pi}\operatorname{Im}G^{\mathrm{R}}(\varepsilon,\xi_p) \tag{15}$$

of the respective Green function (14) for different values of the parameter $W=v_{\mathrm{F}}\kappa/\Delta$ (i.e., virtually the reciprocal correlation length). The energy scale is given in units of Δ (i.e., $E=\varepsilon/\Delta$ and $x=\xi_p/\Delta$).

In the case of well-defined quasiparticles the spectral density is simply $\delta(\varepsilon-\xi_p)$. The results depicted in figures 4 and 5 suggest that at small values of the parameter W (large correlation lengths $\xi \gg v_{\mathrm{F}}/\Delta$) our solution contains no contributions of the quasiparticle type. This fact was noted in [7, 8], where it was demonstrated explicitly that there are no pole contributions to $G(\varepsilon,\xi_p)$ in the approximation of large correlation lengths. At the same time, figures 4 and 5 show that at fairly large values of W (small correlation lengths) the spectral density is represented by a fairly sharp peak at $\varepsilon \propto \xi_p$ corresponding to weakly damped one-electron excitations. The physical meaning of this result is simple. In the limit of $\xi=\kappa^{-1}\to 0$ the random field correlator (1) becomes short-ranged but is not reduced to the common [3, 5] 'white noise' limit. Although in this case all momenta in the integral with respect to Q become important, the scattering amplitude

$$\langle\Delta_Q\Delta_{-Q}\rangle \propto \frac{\Delta^2}{\kappa} \tag{16}$$

so that the effective scattering rate

$$\frac{1}{\tau}\propto 2\pi N_0(\varepsilon_{\mathrm{F}})\frac{\Delta^2}{\kappa}=\frac{\Delta^2}{v_{\mathrm{F}}\kappa}$$
$$=\frac{\Delta}{W}\to 0 \qquad \text{as} \qquad \kappa\to\infty \tag{17}$$

with $N_0(\varepsilon)=1/2\pi v_{\mathrm{F}}$ the one-electron density of states of free electrons. Correspondingly, in the limit of $\kappa\to\infty$ the freedom of the electrons becomes ever greater. This fact is important for the interpretation of the results that are given below. Similar behaviour (as figure 4 shows) appears as ξ_p grows, that is, as one moves away from the Fermi surface.

3. The two-particle Green function and the electromagnetic response

Let us now analyse the two-particle Green function (the vertex part), which determines the frequency dependence of conductivity and the dielectric constant of the system.

We begin by studying the response to a variation of the external scalar potential, $\delta\varphi_{q,\omega}$:

$$\delta G(\varepsilon,\xi_p)=G(\varepsilon,\xi_p)J(\varepsilon,\xi_p;\varepsilon+\omega,\xi_{p+q})G(\varepsilon+\omega,\xi_{p+q})\delta\varphi_{q,\omega} \tag{18}$$

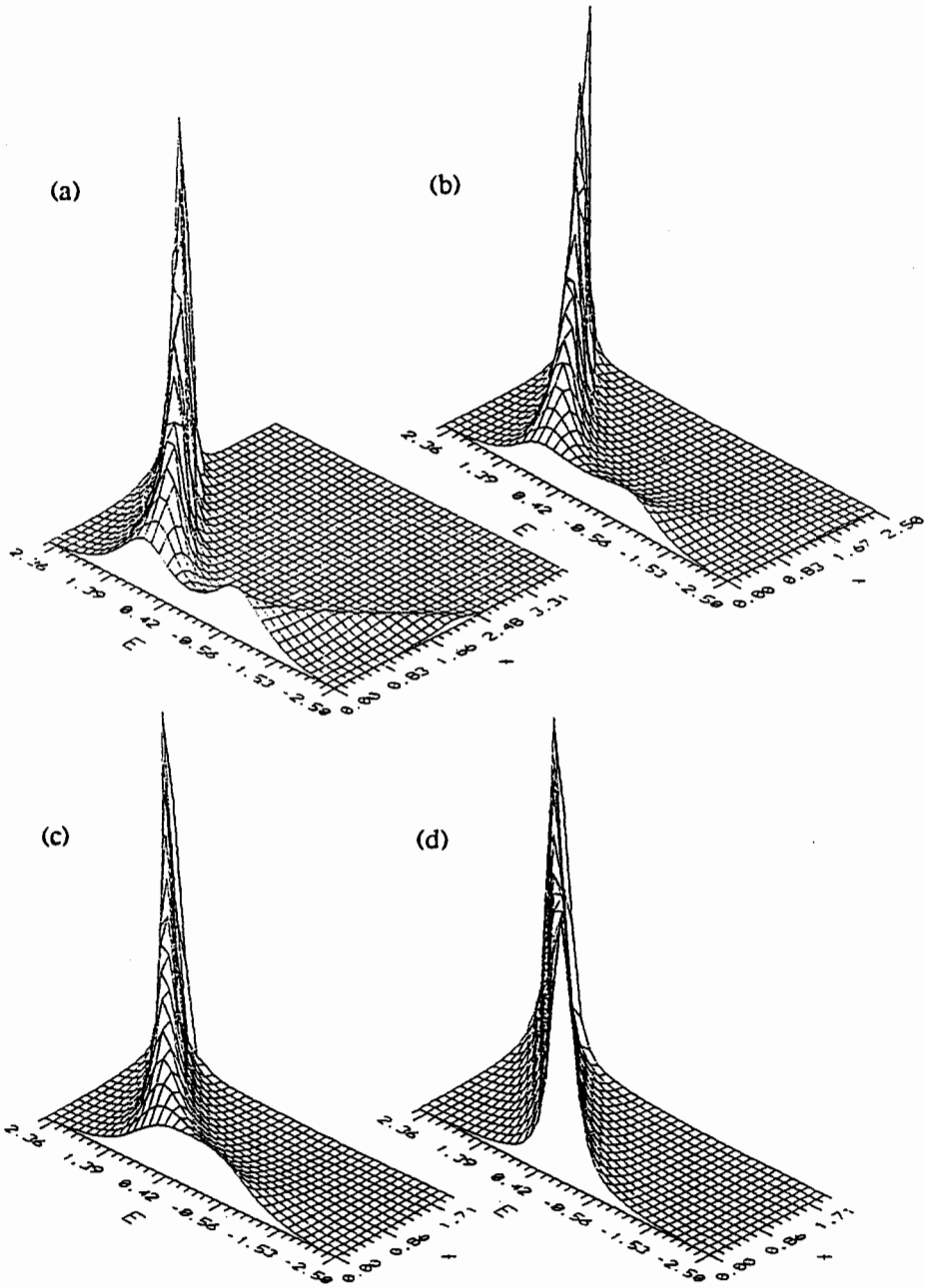

Figure 4. The surfaces of constant spectral density $A(E, x)$: $E = \varepsilon/\Delta$, $x = \xi_p/\Delta$, and $W = v_{pF}/\Delta$. (a) $W = 0.1$, (b) $W = 0.5$, (c) $W = 1.0$, and (d) $W = 5.0$.

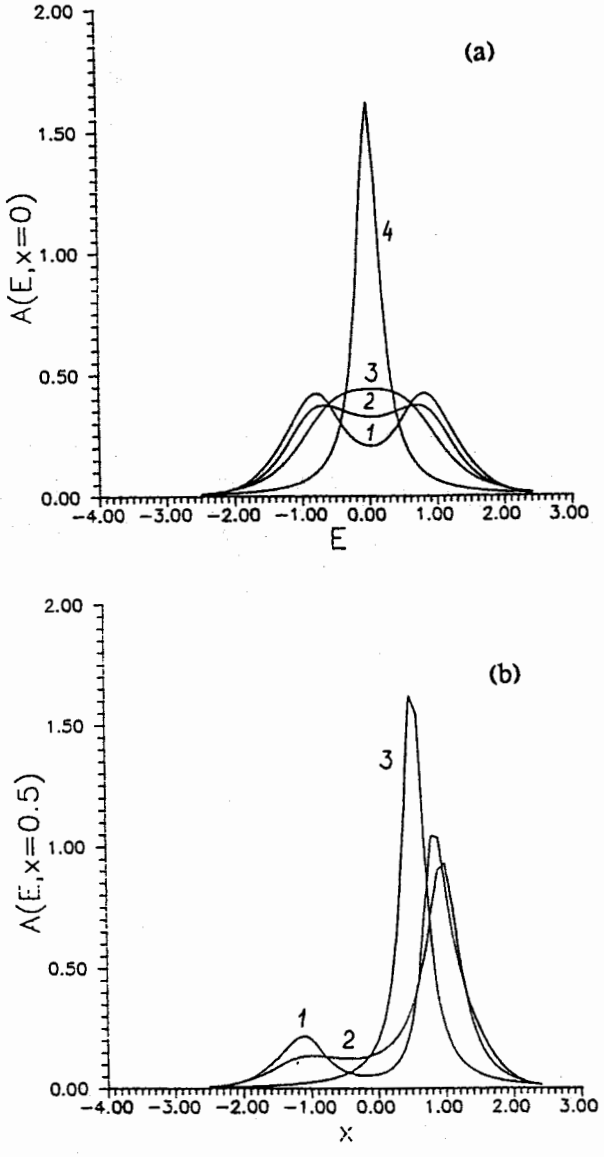

Figure 5. Characteristic cross sections of the surfaces of constant spectral density $A(E,x)$: (a) $x = 0$ at $W = 0.1\,(1)$, $W = 0.5\,(2)$, $W = 1.0\,(3)$, and $W = 5.0\,(4)$; (b) $x = 0.5$ at $W = 0.1\,(1)$, $W = 0.5\,(2)$, and $W = 5.0\,(3)$.

where the vertex part

$$J(\varepsilon,\xi_p;\varepsilon+\omega,\xi_{p+q}) = -\frac{\delta G^{-1}(\varepsilon,\xi_p)}{\delta\varphi_{q,\omega}} \tag{19}$$

for free particles (the free-particle Green function) is determined solely by the charge e.

Equation (6) yields

$$J(\varepsilon,\xi_p;\varepsilon+\omega,\xi_{p+q}) = e + \frac{\delta\Sigma_1(\varepsilon,\xi_p)}{\delta\varphi_{q,\omega}} \equiv e + \mathcal{J}_1(\varepsilon,\xi_p;\varepsilon+\omega,\xi_{p+q}). \tag{20}$$

The problem reduces to calculating the variational derivatives of diagrams of the type depicted in figure 3; the graphs with crossed lines may be ignored because they are taken into account by the respective combinatorial factors at the 'initial' vertexes.

Combining (13) and (14), we introduce the following hierarchy of vertex parts:

$$\begin{aligned} J_1(\varepsilon,\xi_p;\varepsilon+\omega,\xi_{p+q}) &= -\frac{\delta G_1^{-1}(\varepsilon,\xi_p)}{\delta\varphi_{q.\omega}} \\ &= e + \frac{\delta\Sigma_2(\varepsilon,\xi_p)}{\delta\varphi_{q,\omega}} \\ &\equiv e + \mathcal{J}_2(\varepsilon,\xi_p;\varepsilon+\omega,\xi_{p+q}) \end{aligned}$$

$$\begin{aligned} J_{k-1}(\varepsilon,\xi_p;\varepsilon+\omega,\xi_{p+q}) &= -\frac{\delta G_{k-1}^{-1}(\varepsilon,\xi_p)}{\delta\varphi_{q.\omega}} \\ &= e + \frac{\delta\Sigma_k(\varepsilon,\xi_p)}{\delta\varphi_{q,\omega}} \\ &\equiv e + \mathcal{J}_k(\varepsilon,\xi_p;\varepsilon+\omega,\xi_{p+q})\ldots \end{aligned} \tag{21}$$

with $J_{k=0} \equiv J(\varepsilon,\xi_p;\varepsilon+\omega,\xi_{p+q})$. An important assumption is present here, namely, that the variational derivatives of the free-particle Green functions (with contributions $\mathrm{i}v_F\kappa$ in the denominators) are still determined by the 'bare' charge e.

In what follows we will be mainly interested in the vertex of the RA type, with the incoming line of the A (advanced) type and the outgoing of the R (retarded) type. We can try to calculate the corresponding contributions to the variational derivatives $\delta\Sigma_k(\varepsilon,\xi_p)/\delta\varphi_{q,\omega}$ explicitly. Let us consider the simplest diagram for the first-order correction in Δ^2 to the vertex part (figure 6(a)). For the corresponding contribution we easily find that

$$\begin{aligned} &\mathcal{J}_1^{(1)\mathrm{RA}}(\varepsilon,\xi_p;\varepsilon+\omega,\xi_{p+q}) \\ &= \Delta^2\int\frac{\mathrm{d}Q}{2\pi}\,S(Q)G_0^{\mathrm{A}}(\varepsilon,\xi_{p-Q})G_0^{\mathrm{R}}(\varepsilon+\omega,\xi_{p-Q+q}) \\ &= \Delta^2\left[G_0^{\mathrm{A}}(\varepsilon,-\xi_p+\mathrm{i}v_F\kappa) - G_0^{\mathrm{R}}(\varepsilon+\omega,-\xi_{p+q}-\mathrm{i}v_F\kappa)\right]\frac{1}{\omega+v_Fq} \\ &= \Delta^2 G_0^{\mathrm{A}}(\varepsilon,-\xi_p+\mathrm{i}v_F\kappa)G_0^{\mathrm{R}}(\varepsilon+\omega,-\xi_{p+q}-\mathrm{i}v_F\kappa)\left(1+\frac{2\mathrm{i}v_F\kappa}{\omega+v_Fq}\right) \end{aligned} \tag{22}$$

where we have used the identity

$$G_0^{\mathrm{A}}(\varepsilon,\xi_p)G_0^{\mathrm{R}}(\varepsilon+\omega,\xi_{p+q}) \equiv \left[G_0^{\mathrm{A}}(\varepsilon,\xi_p) - G_0^{\mathrm{R}}(\varepsilon+\omega,\xi_{p+q})\right]\frac{1}{\omega-v_Fq}.$$

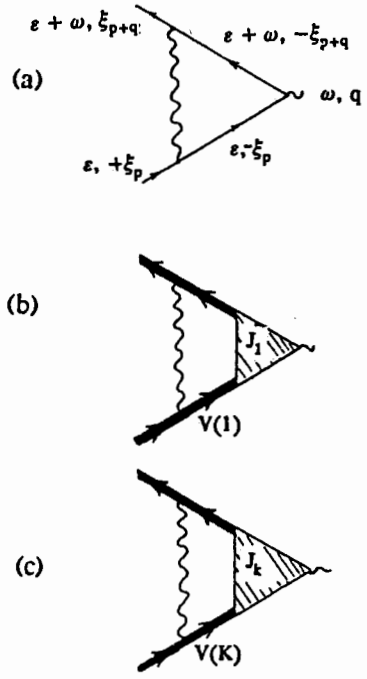

Figure 6. The simplest diagrams for the vertex part.

'Dressing' all the internal electron lines and employing the identity

$$G^{A}(\varepsilon,\xi_p)G^{R}(\varepsilon+\omega,\xi_{p+q}) \equiv \left[G^{A}(\varepsilon,\xi_p)-G^{R}(\varepsilon+\omega,\xi_{p+q})\right] \times \frac{1}{\omega - v_F q - \Sigma_1^{R}(\varepsilon+\omega,\xi_{p+q}) + \Sigma_1^{A}(\varepsilon,\xi_p)} \tag{23}$$

we obtain the contribution of the diagram in figure 6(b) in the following form:

$$J_1^{RA}(\varepsilon,\xi_p;\varepsilon+\omega,\xi_{p+q}) = \Delta^2 G_1^{A}(\varepsilon,\xi_p)G_1^{R}(\varepsilon+\omega,\xi_{p+q}) \times \left(1+\frac{2iv_F^{-1}\kappa}{\omega+v_F q-\Sigma_2^{R}(\varepsilon+\omega,\xi_{p+q})+\Sigma_2^{A}(\varepsilon,\xi_p)}\right) \times J_1^{RA}(\varepsilon,\xi_p;\varepsilon+\omega,\xi_{p+q}) \tag{24}$$

where we have assumed that an extra interaction line simply transforms the respective self-energy parts $\Sigma_1^{R,A}$ into $\Sigma_2^{R,A}$ in the spirit of the procedure discussed in section 2. A straightforward generalization for the contribution of the diagram depicted in

figure 6(c), with the lines dressed according to the rules suggested above, has the form

$$\mathcal{J}_k^{RA}(\varepsilon,\xi_p;\varepsilon+\omega,\xi_{p+q}) = \Delta^2 v(k) G_k^A(\varepsilon,\xi_p) G_k^R(\varepsilon+\omega,\xi_{p+q}) \times \left\{1+\frac{2iv_F\kappa\, k}{\omega-(-1)^k\quad v_F q-\Sigma_{k+1}^R(\varepsilon+\omega,\xi_{p+q})+\Sigma_{k+1}^A(\varepsilon,\xi_p)}\right\} \times J_k^{RA}(\varepsilon,\xi_p;\varepsilon+\omega,\xi_{p+q}). \tag{25}$$

The main feature here is the absence of terms of the $iv_F\kappa$ type in the denominator in the second term within the braces, which in the summation procedure discussed in section 1 were "shifted" from the proper self-energy parts to the corresponding free-particle Green functions.

In addition to the above assumptions concerning the properties of variational derivatives of the free-particle Green functions, this procedure forms the basis of the suggested method. This procedure does indeed take into account all the Feynman diagrams emerging in the problem, but it is based on important assumptions concerning the structure of separate terms in the series. Below we suggest additional arguments in favour of the validity of these assumptions.

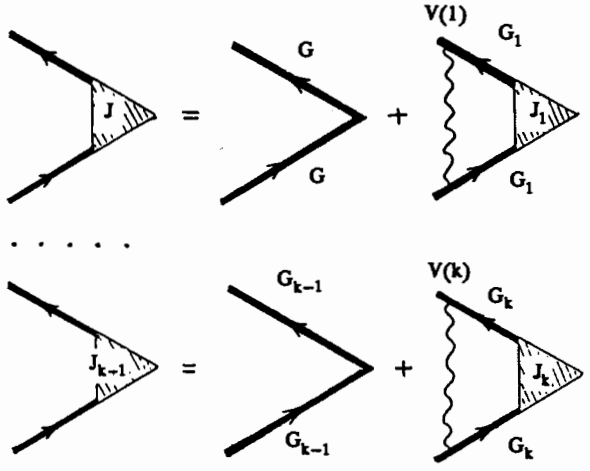

Figure 7. Diagrammatic representation of the equations for the vertex hierarchy.

As a result we arrive at the following fundamental recurrence relations for the vertex part:

$$J_{k-1}^{RA}(\varepsilon,\xi_p;\varepsilon+\omega,\xi_{p+q}) = e+\Delta^2 v(k) G_k^A(\varepsilon,\xi_p) G_k^R(\varepsilon+\omega,\xi_{p+q}) J_k^{RA}(\varepsilon,\xi_p;\varepsilon+\omega,\xi_{p+q}) \times \left\{1+\frac{2iv_F\kappa k}{\omega-(-1)^k v_F q+v(k+1)\Delta^2\left[G_{k+1}^A(\varepsilon,\xi_p)-G_{k+1}^R(\varepsilon+\omega,\xi_{p+q})\right]}\right\}. \tag{26}$$

Diagrammatically these relations are depicted in figure 7

Further analysis can easily be done numerically: we truncate the continuous fraction for the G-function at a distant 'storey' assuming that the corresponding Σ_k is zero and that $J_k = e$ and then 'raise' to the physical limit of $k = 0$. One can easily verify that on the limit of $\kappa \to 0$ the suggested procedure leads to the series that was summed analytically in [7, 8].

To find the frequency dependence of the conductivity we can use the general relations discussed in [18, 19]. The conductivity is expressed in terms of the density–density retarded response function (the polarization operator) $\chi^{R}(q,\omega)$ as follows:

$$\sigma(\omega) = e^2 \lim_{q\to 0}\left(-\frac{i\omega}{q^2}\right)\chi^{R}(q,\omega). \tag{27}$$

The dielectric constant can also be easily found:

$$\mathrm{Re}\,\varepsilon(\omega) - 1 = -\frac{4\pi}{\omega}\,\mathrm{Im}\,\sigma(\omega) \qquad \mathrm{Im}\,\varepsilon(\omega) = \frac{4\pi}{\omega}\,\mathrm{Re}\,\sigma(\omega).$$

The general expression for $\chi^{R}(q,\omega)$ has the following form [18, 19]:

$$\chi^{R}(q,\omega) = \int d\varepsilon\,\{[f(\varepsilon+\omega) - f(\varepsilon)]\Phi^{RA}(\varepsilon,q,\omega)\} + \int d\varepsilon\,[f(\varepsilon)\Phi^{RR}(\varepsilon,q,\omega) - f(\varepsilon+\omega)\Phi^{AA}(\varepsilon,q,\omega)] \tag{28}$$

where $f(\varepsilon)$ is the Fermi distribution function, and the two-particle Green functions Φ^{RA}, Φ^{RR}, and Φ^{AA} are represented by loop diagrams of the type depicted in figure 8.

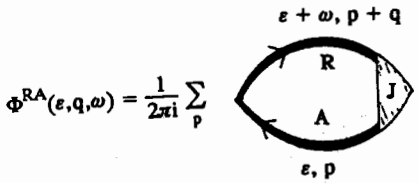

$\Phi^{RA}(\varepsilon,q,\omega) = \frac{1}{2\pi i}\sum_{p}$

Figure 8. Diagrammatic representation of $\Phi^{RA}(\varepsilon,q,\omega)$.

For $T = 0$ and $\omega \ll \varepsilon_F$ we have [19]

$$\chi^{R}(q,\omega) = \omega[\Phi^{RA}(0,q,\omega) - \Phi^{RA}(0,0,\omega)]. \tag{29}$$

We note the existence of an important relation of the Ward identity type [18, 19] that reflects the law of conservation of the number of particles (and is valid for $\omega \ll \varepsilon_F$):

$$\Phi^{RA}(0,0,\omega) = -\frac{N(\varepsilon_F)}{\omega} \tag{30}$$

with $N(\varepsilon_F)$ the exact (renormalized) density of states at the Fermi level. This equation was employed in deriving (29) and can be used to directly monitor the suggested recurrence procedure of calculating the two-particle Green function.

4. Results and discussion

As noted in [9], the recurrence procedure for finding the one-particle Green function (the density of states) converges very rapidly; a typical calculation time for the density of states at a given energy (with a high accuracy) amounts to less than one minute when a standard IBM PC/AT is used (if one starts from the 'storey' with $k = 50$–100). The situation is more complicated when conductivity and the dielectric constant are calculated and the procedure is more sensitive to the choice of parameters of interest to us. In the main section of the frequency interval, $0.5\Delta < \omega < 3\Delta$, and for intermediate values of $\xi = \kappa^{-1}$ ($0.2\Delta < v_F\kappa < 2\Delta$), satisfactory convergence is achieved for $k < (2\text{–}5) \times 10^2$ and the calculation time for conductivity at a fixed frequency amounts to several minutes. Outside the specified intervals the convergence grows markedly worse and becomes especially poor in the limit of very low frequencies and in the case of extremely large correlation lengths (note that in the latter case the exact analytical solution can be used [7, 8]).

The reliability of the suggested recurrence procedure can be verified by directly checking the validity of the exact formula (30). In doing so, one finds that calculating $N(\varepsilon_F)$ in terms of the two-particle Green function $\Phi^{RA}(0,\omega)$ yields (at least for $\omega \ll \Delta$) a result agreeing perfectly with that of $N(\varepsilon_F)$ calculated in terms of the one-electron Green function for various values of parameter κ. This can, apparently, serve as a strong indication that the employed method is correct, which makes it possible to speak of an 'exact' solution.

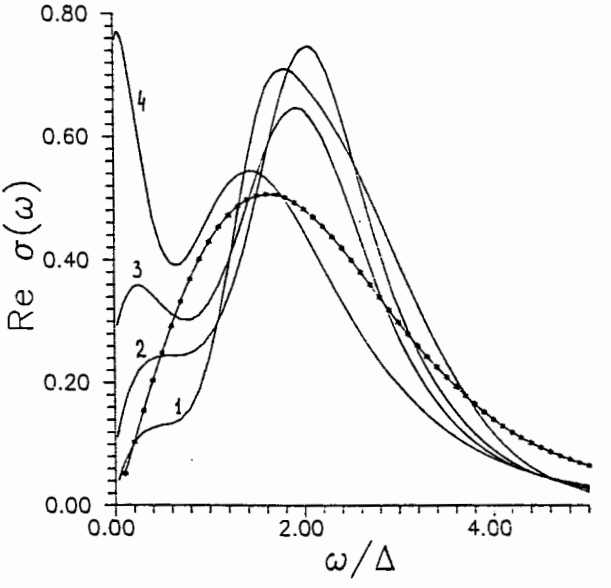

Figure 9. The frequency dependence of the real part of conductivity in the case of incommensurate fluctuations: $W = 0.1(1)$, $W = 0.5(2)$, $W = 1.0(3)$, and $W = 2.0(4)$; the $*$ stand for the exact solution at $W = 0$ [7, 8].

In figure 9 we give the results of calculating the frequency dependence of

conductivity for the case of incommensurate short-range order fluctuations. The conductivity is given everywhere in units of $\omega_p^2/4\pi\Delta$ (there is an error in [15] concerning this scale—the presence of an extra factor of 2 in the denominator), with ω_p the plasma frequency, and the correlation length is determined by parameter $W = v_F\kappa/\Delta$. For the sake of comparison we also give the results of an exact analytical solution in the limit of $W \to 0$ [7, 8]. One can clearly see the successive degradation of the intensity of absorption through the pseudogap as ξ decreases (or W grows). For small W (or large ξ), the localized behaviour of $\mathrm{Re}\,\sigma(\omega)$ in the low-frequency region, $\mathrm{Re}\,\sigma(\omega \to 0) \to 0$, manifests itself in a way that is qualitatively similar to the behaviour discovered in another model [5]. There appears a characteristic additional maximum in the conductivity similar to the maximum obtained in the problem of conductivity in a system of δ-correlated impurities ('white noise') [5]. As W grows, the apparent localized behaviour disappears, changing to the Drude-like behaviour characteristic of free electrons. Thus, our model demonstrates an 'effective' Anderson transition, notwithstanding its one-dimensional nature.

Though this may seem to be paradoxical behaviour, it has a simple qualitative explanation based on the decrease of the effective scattering amplitude in the limit of large κ, a property discussed in section 2. Naturally, the frequency region where localization effects manifest themselves is drastically narrowed in the process and for all practical purposes disappears as the electrons' freedom increases. It is in this sense that we can speak of an effective Anderson transition.

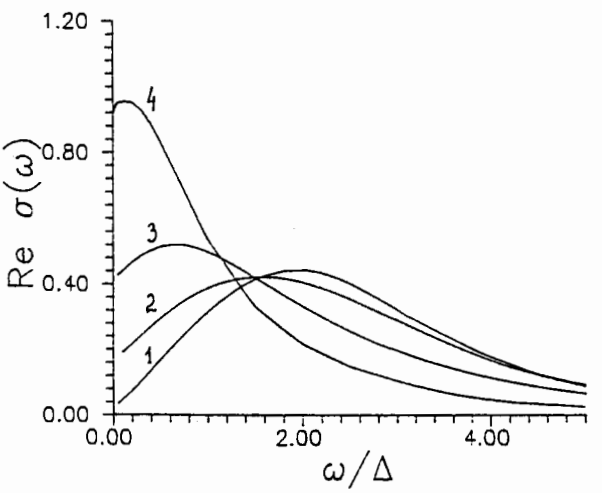

Figure 10. The frequency dependence of the real part of conductivity in the case of commensurate fluctuations: $W = 0.5\,(1)$, $W = 2.0\,(2)$, $W = 4.0\,(3)$, and $W = 8.0\,(4)$.

Figure 10 demonstrates the results of calculating $\mathrm{Re}\,\sigma(\omega)$ for the case of commensurable short-range order fluctuations. Qualitatively, the picture noticeably differs from the incommensurate case: there is no additional maximum in the low-frequency region for small W. At the same time, the effective Anderson transition from the localized behaviour to the Drude-like becomes even more evident.

The suggested method can also be used to establish the frequency behaviour of the dielectric constant $\mathrm{Re}\,\varepsilon(\omega)$. The corresponding results are given in [15].

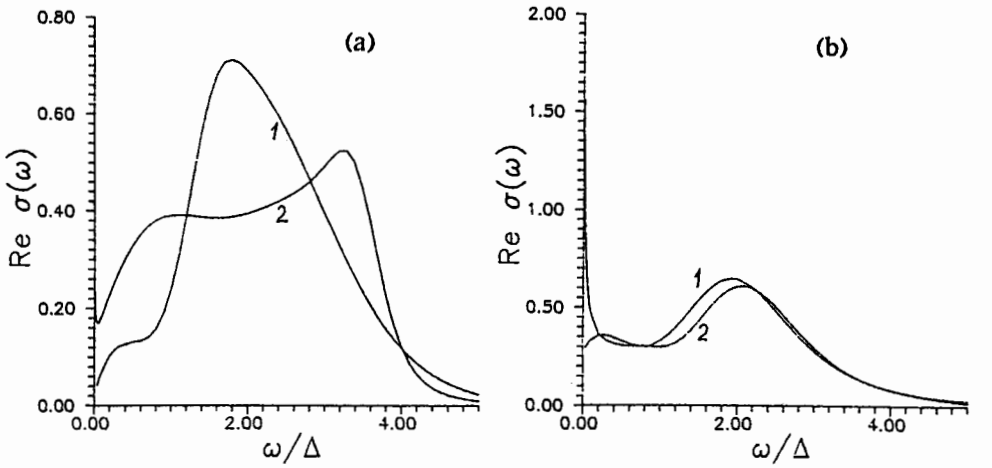

Figure 11. Comparison of the results of an 'exact' analysis with those obtained in the 'ladder' approximation: (a) $W = 0.1$ (1) the 'exact' solution and (2) the 'ladder' approximation; (b) $W = 1.0$ (1) the 'exact' solution and (2) the 'ladder' approximation.

It is interesting to compare the results of an 'exact' analysis with those of calculations carried out in the standard 'ladder' approximation, that is, an approximation that does not allow for diagrams with crossed interaction lines. In our method the transition to the 'ladder' approximation is very simple: one needs only to set all combinatorial factors $v(k)$ equal to unity (in both the incommensurate and the commensurate case). Figure 11 depicts the most characteristic curves for $\mathrm{Re}\,\sigma$ plotted against ω for the incommensurate case. The reader can clearly see that for small W (figure 11(a)) the 'ladder' approximation gives a behaviour that drastically differs from 'exact'. Localized behaviour is distinctly absent from the low-frequency region, which is natural since localization is determined by diagrams with crossed interaction lines [18]. At the same time, for fairly large W (figure 11(b)) in the main frequency region the 'ladder' approximation yields results that are close to 'exact'. However, for low frequencies here, too, distinct discrepancies emerge: all tendency to localization vanishes. The same behaviour is observed in the commensurate case.

Note that the suggested method can also be easily used to analyse the one-dimensional model with a Gaussian random field correlator in the form of a simple Lorentzian centred at zero momentum transfer, $Q \approx 0$. Naturally, this model generates a density of states with a characteristic 'tail' at the band's edge. However, calculating the two-particle Green function yields trivial free behaviour in this model. For instance, it can easily be verified that $\mathrm{Re}\,\varepsilon(\omega) = 1 - \omega_p^2/\omega^2$. This result is an obvious corollary of the absence (in the one-dimensional case) of dissipation in scattering with low momentum transfer, $Q \ll 2p_F$. The electrons simply re-scatter near $\pm p_F$, the endpoints of the 'Fermi line'. Current dissipation requires scattering by $Q \sim 2p_F$,

which makes the electrons hop from one endpoint of the Fermi line to the other.

5. Conclusion

We have proposed an effective recurrence procedure for calculating the two-particle Green function in a one-dimensional model with a Gaussian random field of a special type that can describe short-range order fluctuations in systems of the Peierls type [8, 9] and, possibly, in high-T_c systems [15]. The procedure allows for all the Feynman diagrams that appear in the given problem and in this sense is 'exact', although it is based on certain assumptions concerning the structure of the terms in the perturbation series. The reliability of these assumptions is verified by the meaningfulness of the limiting cases of $\kappa \to 0$ and $\kappa \to \infty$ and by the fact that the exact 'Ward' identity holds for all values of κ.

The general pattern of the evolution of the frequency dependence of conductivity for various values of the short-range order correlation length describes absorption through a pseudogap and localized behaviour in the region of low ω and W. As W grows (or the correlation length decreases) an 'effective' Anderson transition occurs in the system, and this would seem to explain the drop in the scattering amplitude and the gradual transition to 'free' particles as W grows. From the practical viewpoint the frequency range where localization manifests itself narrows drastically and disappears. Such behaviour may lead to interesting consequences in real quasi-one-dimensional systems.

References

[1] Halperin B I 1968 *Adv. Chem. Phys.* **13** 123
[2] Erdős P and Herndon R C 1978 *Adv. Phys.* **31** 65
[3] Berezinskii V L 1974 *Sov. Phys.-JETP* **38** 620
[4] Abrikosov A A and Ryzhkin I A 1978 *Adv. Phys.* **27** 147
[5] Gogolin A A 1982 *Phys. Rep.* **86** 1
Gogolin A A 1988 *Phys. Rep.* **166** 269
[6] Abrikosov A A, Gor'kov L P and Dzyaloshinskii I E 1963 *Methods of Quantum Field Theory in Statistical Physics* (New York: Prentice-Hall)
[7] Sadovskii M V 1974 *Sov. Phys.-JETP* **39** 845
[8] Sadovskii M V 1975 *Sov. Phys. Solid State* **16** 1632
[9] Sadovskii M V 1979 *Sov. Phys.-JETP* **50** 989
[10] Wonneberger W and Lautenschlager R 1976 *J. Phys. C: Solid State Phys.* **9** 2865
[11] Wonneberger W 1977 *J. Phys. C: Solid State Phys.* **10** 1073
[12] Munz K M and Wonneberger W 1990 *Z. Phys.* **79** 15
[13] Kampf A and Schrieffer J R 1990 *Phys. Rev.* B **41** 6399
[14] Kampf A and Schrieffer J R 1990 *Phys. Rev.* B **42** 7967
[15] Sadovskii M V and Timofeev A A 1991 *Superconductivity: Physics, Chemistry, Technology* **4** 11
[16] Lee P A, Rice T M and Anderson P W 1973 *Phys. Rev. Lett.* **31** 462
[17] Elyutin P V 1977 *Opt. Spectrosc. (USSR)* **43** 318
[18] Maleev S V and Toperverg B P 1975 *Sov. Phys.-JETP* **42** 734
[19] Vollhardt D and Wolfle P 1980 *Phys. Rev.* B **22** 4666